




Fusobacterium nucleatum mediates endothelial damage and increased permeability following single species and polymicrobial infection

Cher Farrugia^{1,2} | Graham P. Stafford¹ | Ashley F. Gains¹ | Antonia R. Cutts¹ |
Craig Murdoch¹ 

¹School of Clinical Dentistry, University of Sheffield, Sheffield, UK

²Bristol Dental School, University of Bristol, Bristol, UK

Correspondence

Craig Murdoch, School of Clinical Dentistry, University of Sheffield, Sheffield, S10 2TA, UK.

Email: c.murdoch@sheffield.ac.uk

Abstract

Background: Numerous lines of evidence link periodontal pathobionts and their virulence factors with endothelial damage. Most research has been conducted using single species infections at the exclusion of other periodontal microorganisms that have been identified in vascular tissue. Here, we assessed endothelial infection with either single or mixed periodontal species infection and examined their effect on endothelial damage and permeability.

Methods: Cell surface abundance of platelet endothelial cell adhesion molecule-1 (PECAM-1) or endothelial permeability following infection with *Porphyromonas gingivalis*, *Fusobacterium nucleatum* subspecies (ssp) *nucleatum*, ssp *polymorphum* or *Tannerella forsythia* as single or mixed species infection was determined by flow cytometry and a fluorescent dextran permeability assay. Zebrafish embryos were infected systemically with either single or mixed species with mortality and disease measured over time.

Results: *F. nucleatum* ssp *nucleatum*, ssp *polymorphum* and *P. gingivalis* significantly reduced PECAM-1 abundance in single species infection, whereas *T. forsythia* had no effect. *F. nucleatum* ssp *polymorphum* caused considerable mortality and morbidity in a zebrafish systemic infection model. Polymicrobial infection underscored the virulence of *F. nucleatum* ssp *polymorphum* in particular with increased endothelial cell death and reduced PECAM-1 abundance in co-infection studies with this organism. When injected systemically into zebrafish in polymicrobial infection, fluorescently labeled bacteria were distributed throughout the vasculature and cardiac region where, in some instances, they co-localized with each other.

Conclusions: These data provide further evidence on the effects of *F. nucleatum* on endothelium adhesion molecule abundance and permeability while also highlighting the importance of performing polymicrobial infection to study the

This is an open access article under the terms of the [Creative Commons Attribution-NonCommercial](https://creativecommons.org/licenses/by-nc/4.0/) License, which permits use, distribution and reproduction in any medium, provided the original work is properly cited and is not used for commercial purposes.

© 2022 The Authors. *Journal of Periodontology* published by Wiley Periodicals LLC on behalf of American Academy of Periodontology.



molecular mechanisms associated with periodontal pathogen-induced vascular damage.

KEYWORDS

atherosclerosis, cardiovascular diseases, host–microbial interactions, periodontitis, *Porphyromonas gingivalis*

1 | INTRODUCTION

Periodontal infection increases the risk of cardiovascular disease and coronary heart disease,¹ with epidemiological studies associating periodontal disease with both clinical and subclinical atherosclerotic vascular disease.² In patients displaying periodontitis, periodontal pathogens can enter the bloodstream through areas of inflamed and ulcerated periodontal tissue^{3,4} or indirectly through a "Trojan-horse" approach where bacteria internalized by immune cells are carried and then released into the circulation.⁵ Molecular approaches have identified the presence of periodontal pathogens in both healthy and diseased vasculature tissue including *P. gingivalis*,^{3,6–8} *Fusobacterium nucleatum*,^{8–10} and *T. forsythia*.^{3,7,9}

Out of all the periodontal pathobionts thus far identified in vascular tissues, it is the interactions between endothelial cells and *P. gingivalis* that have been most frequently studied.^{11,12} Platelet endothelial cell adhesion molecule-1 (PECAM-1/CD31) is responsible for maintaining vascular integrity at endothelial cell-cell junctions, and its cell surface cleavage or reduction in expression leads to disruption of cell adhesive contacts and increased vascular permeability.¹³ Previous studies have reported gingipain-dependent cleavage of PECAM-1 upon *P. gingivalis* infection.^{14,15} A decrease in endothelial cell PECAM-1 abundance has also been reported following *F. nucleatum* infection¹⁶; while effects of *T. forsythia* on this adhesion molecule have not been examined. In addition, changes in vascular integrity following *F. nucleatum* infection have been attributed to *Fusobacterium* adhesin A (FadA) adherins by binding to vascular endothelial (VE)-cadherin.¹⁷ Although periodontal pathobionts are generally found associated with one another within a microbial biofilm and not as solitary organisms,¹⁸ assessment of polymicrobial interactions and their effects on endothelial cells is infrequent. Polymicrobial interactions can alter the pathogenicity of periodontal pathogens. For example, *F. nucleatum* has been shown to enhance the invasion of *P. gingivalis* into aortic endothelial cells in vitro,¹⁹ while in vivo polymicrobial infections elicit distinct inflammatory responses and increased aortic oxidative stress.^{20–22}

This study aimed to compare the effects of single species infection of endothelial cells with *P. gingivalis*, *F. nucleatum*, and *T. forsythia* in terms of cell surface PECAM-1 adhesion molecule abundance and endothelial permeability, and to further investigate whether these effects are altered in polymicrobial infections. We show that, in single species infection, *P. gingivalis* and *F. nucleatum* but not *T. forsythia* infection contribute toward endothelial damage through increased permeability and decreased intercellular PECAM-1 abundance in human microvascular endothelial cells (HMEC-1) endothelial cells. *F. nucleatum* was also virulent in a zebrafish systemic infection model and in in vitro polymicrobial infections. These data highlight not only the significance of *F. nucleatum* in mediating changes in the vasculature, but also the importance of polymicrobial infection and interspecies interactions when assessing the effects of periodontal pathogens on the vasculature.

2 | MATERIALS AND METHODS

2.1 | Microbial culture

Wild-type strains *P. gingivalis* W83, *F. nucleatum* subspecies (ssp) *nucleatum* (ATCC 25586), and ssp *polymorphum* (ATCC 10953) were maintained on Fastidious Anaerobe (FA)* agar plates supplemented with 5% v/v oxylated horse blood†. Isogenic $\Delta K/R$ -ab (*kgp* Δ 598-1732::*Tc*^R *rgpA*::*Cm*^R *rgpBA*410-507::*EmR*; provided by Prof. Jan Potempa, Jagiellonian University, Kraków, Poland) was grown on FA plates supplemented with 1 μ g/ml tetracycline, while *T. forsythia* (ATCC43037) was cultured on FA plates supplemented with 1% N-acetylmuramic acid (NAM)‡ in addition to oxalated horse blood. Agar and broth microbial cultures were incubated at 37°C in an anaerobic chamber with an atmosphere of 80% N₂, 10% CO₂ and 10% H₂. For use in experiments, strains were grown as broth cultures anaerobically for 18 h, adjusted to an optical density (OD₆₀₀) equal to 0.1 with fresh broth then cultured until log phase.

* Neogen, Ayr, UK

† Oxoid Ltd., Basingstoke, UK

‡ Merck Life Sciences, Gillingham, UK



Bacteria were then harvested by centrifugation at 8000 g for 3 min, washed with phosphate buffered saline (PBS) and resuspended at the required density.

2.2 | Endothelial cell culture

Immortalized HMEC-1²³ were grown in MCDB131 medium supplemented with 10 ng/ml epidermal growth factor[‡], 1 µg/ml hydrocortisone[‡], 10% fetal calf serum[‡], and 2 mM L-glutamine[‡] and cultured at 37°C, 5% CO₂ in a humidified incubator.

2.3 | Flow cytometry

HMEC-1 cells were seed at 4×10^5 cells per well and cultured to confluence in six-well plates then infected with either single species *P. gingivalis* W83, *P. gingivalis* ΔK/R-ab; *F. nucleatum* subspecies *nucleatum* or ssp *polymorphum* or *T. forsythia* or in mixed cultures of these organisms just before addition to the endothelial monolayers. Multiplicity of infection (MOI) was achieved by counting the total number of HMEC-1 cells in one well following detachment, then adding the required number of bacteria to the other confluent HMEC-1-containing wells to reach MOI of 10, 20, or 100. Infected cells were then cultured for 1.5 h at 37°C in serum-free MCDB131 medium. MCDB131 medium alone was used as uninfected controls. Following infection, HMEC-1 monolayers were washed, removed from plates using 0.02% ethylenediaminetetraacetic acid[‡] for 20 min and resuspended in 100 µl fluorescence activated cell sorting (FACS) buffer (0.1% bovine serum albumin [BSA][‡], 0.1% sodium azide[‡] in PBS). Phycoerythrin-Cyanine7-conjugated anti-human CD31 (clone MW59)[§] or conjugated isotype IgG[§] control was added for 45 min on ice. Cells were washed and resuspended in FACS buffer, 3 µl of cell viability dye TO-PRO-3[§] (1 mg/ml) was added to each sample to exclude dead cells and assess cell viability, and then cells were analyzed using a LSRII flow^{||} cytometer. FlowJo software^{||} was used to calculate the normalized median fluorescence index (nMFI).

2.4 | Fluorescent dextran endothelial permeability assay

A fluorescent dextran permeability assay was performed as previously described.²⁴ Fibronectin-coated (10 µg/ml) Millicell hanging cell culture inserts[‡] were seeded with

1×10^5 HMEC-1 cells and grown until confluent then incubated with bacteria for 1.5 h using a MOI 100 at 37°C in serum-free medium. Inserts without cells or HMEC-1 monolayers alone were used as controls. Solutions were removed, inserts transferred to a new plate containing 500 µl supplemented MCDB131 and 450 µl supplemented MCDB131 containing 65 µg/ml 70 kDa fluorescent dextran[§] was added to the upper compartment of the insert. Dextran leakage through the cell monolayer to the bottom well was monitored hourly for a 5-h period by aspirating 250 µl medium from the bottom well and measuring dextran fluorescence at 494 nm excitation, 521 nm emission. The aspirated volume was replaced with fresh supplemented MCDB131 for further readings.

2.5 | Zebrafish larvae systemic infection model

Zebrafish maintenance and experimental work were carried out in accordance with UK Home Office regulations and UK Animals (Scientific Procedures) Act 1986 and under Project Licence P1A4A7A5E (Dr Simon Johnston) using zebrafish embryos under 5 days post fertilization (dpf). London wild-type (LWT) zebrafish were maintained in E3 medium at 30°C according to standard protocols.

For Kaplan-Meier analysis, LWT zebrafish larvae at 30 h post fertilization (hpf) were anesthetized using tricaine (0.02% (w/v) 3-amino benzoic acid ester tricaine/MS-322[§], positioned in a solution of 3% (w/v) methylcellulose[§] in E3 medium and 2 nl of *F. nucleatum* ssp *polymorphum*, suspended at 1×10^2 , 5×10^2 , and 2×10^3 colony forming units (CFU)/ml, injected systemically using a microcapillary needle via direct microinjection into common cardinal vein. PBS was used as control. Injections using 4% paraformaldehyde-fixed or heat-killed (60°C for 30 min) *F. nucleatum* ssp *polymorphum* (2×10^3 CFU/ml; loss of bacterial viability was confirmed by agar culture) were also performed to assess effects of non-viable bacteria. Zebrafish viability was assessed by examining the presence of a heartbeat and blood flow within the circulation and disease by presence of edema at 24, 48, and 72 hpi.

To visualize single species systemic infection, *F. nucleatum* ssp *polymorphum* was fluorescently labeled with 0.4 µg/ml 5-(and-6)-carboxyfluorescein, succinimidyl ester (excitation 494 nm, emission 518 nm)[§] in PBS for 15 min with shaking at 4°C. Then, 2 nl of 2×10^3 CFU/ml FAM-labeled *F. nucleatum* ssp *polymorphum* was injected into the common cardinal vein of 72 hpf kdrl:mCherry transgenic zebrafish as previously described and imaged 2 hpi using Lightsheet microscopy (Zeiss). For multispecies systemic infection, single species microbial cultures were initially fluorescently labeled as follows; *P. gingivalis* with

[§] ThermoFisher Scientific, Waltham, MA

^{||} BD Biosystems, Franklin Lakes, NY



0.4 $\mu\text{g/ml}$ 5-(and-6)-carboxyfluorescein, succinimidyl ester (excitation 494 nm, emission 518 nm), *F. nucleatum* ssp *polymorphum* with 5 μM Red CMPTX[§] (excitation 577 nm, emission 602 nm) and *T. forsythia* with Deep Red Cell Tracker[§] (excitation 630 nm, emission 650 nm). Labeled bacteria were washed with PBS, mixed at 1:1:1 ratio and 2 nl of a 2×10^3 CFU/ml bacterial suspension injected into the common cardinal vein of 48 hpf nares wild-type zebrafish embryos and imaged using Lightsheet[¶] microscopy at 2 hpi. Additionally, zebrafish were fixed with 4% paraformaldehyde, wax-embedded, and 5 μm sections stained with hematoxylin and eosin.

2.6 | Statistical analysis

Data are presented as mean \pm standard deviation (SD) from at least three independent experiments carried out in triplicate except for flow cytometry data where nMFI (normalized median fluorescence index) was used. Differences between two groups were assessed using either Students *t*-test or Mann Whitney U Test, whilst differences between group data was assessed using one-way analysis of variance (ANOVA) followed by Tukey's post-hoc multiple comparison test. All tests were carried out using GraphPad Prism v9.3.1[#], and statistical significance was assumed at $p < 0.05$.

3 | RESULTS

3.1 | *F. nucleatum* infection decreases PECAM-1 abundance and increases permeability of HMEC-1 monolayers

Previous studies have shown that *P. gingivalis* can cleave PECAM-1^{14,15} and that this is mediated by gingipains. We therefore examined if HMEC-1 infection with other periodontal pathogens such as *F. nucleatum* and *T. forsythia* can also exert their effects on intercellular PECAM-1. Assessment of PECAM-1 abundance on viable HMEC-1 cells by flow cytometry showed infection with wild-type *P. gingivalis* strain W83 (Figure 1A), *F. nucleatum* subspecies *nucleatum* (Figure 1B) and ssp *polymorphum* (Figure 1C) was significantly decreased at MOI 100 compared to untreated controls. In contrast, the *P. gingivalis* gingipain-null mutant (K/R-ab) or *T. forsythia* did not alter cell surface levels of PECAM-1 at any MOI tested compared to controls (Figure 1D,E). Similarly, *P. gingivalis* W83, *F. nucleatum* ssp *nucleatum* or ssp *polymorphum* infection

at MOI 100 significantly decreased the permeability of HMEC-1 endothelial monolayers compared to uninfected controls, whereas infection with K/R-ab and *T. forsythia* did not alter HMEC-1 permeability (Figure 1F).

3.2 | *F. nucleatum* ssp *polymorphum* displays virulence in vivo with increased mortality, edema, and disease in a dose-dependent manner

F. nucleatum ssp *polymorphum* was injected systemically in to LWT zebrafish embryos and its effect on zebrafish embryo morbidity assessed. The *polymorphum* ssp was selected because it showed increased pathogenicity in the in vitro PECAM-1 abundance assay compared to ssp *nucleatum*. *F. nucleatum* ssp *polymorphum* displayed a dose-dependent increase in zebrafish mortality when examined by Kaplan-Meier survival analysis with significantly more death ($66\% \pm 7\%$; $p = 0.027$) observed when zebrafish were injected with 2×10^3 CFU/ml at 72 hpi than uninfected controls ($87\% \pm 4\%$) (Figure 2A). *F. nucleatum* ssp *polymorphum* injection resulted in marked cardiac and yolk edema compared to PBS injected controls (Figure 2B).

When zebrafish embryos were stratified into disease status, systemic injection with *F. nucleatum* ssp *polymorphum*, at all concentrations tested, resulted in a significant increase in the number of zebrafish displaying symptoms of disease (i.e., dead + edematous) compared to PBS injected controls over a period of 72 h ($p < 0.01$). In addition, the numbers of zebrafish classified as diseased (dead + edematous) increased in both a time- and dose-dependent manner (Figure 2C–E) compared to infected but otherwise healthy and viable zebrafish. The presence of intravascular *F. nucleatum* ssp *polymorphum* was confirmed following systemic injection of fluorescently labeled bacteria into 72 hpf kdrl:mCherry transgenic zebrafish (Figure 2F,G). Lightsheet imaging at 2 hpi shows the presence of *F. nucleatum* ssp *polymorphum* in the cardiac and systemic vasculature by co-localization with the mCherry-labeled endothelium (Figure 2F). This co-localization is further highlighted by orthogonal views of the cardiac tissue (Figure 2G).

The pathogenicity of *F. nucleatum* ssp *polymorphum* was significantly reduced following heat treatment or paraformaldehyde fixation compared to wild-type bacteria in terms of overall survival after 72 h (Figure 3A). Moreover, the levels of zebrafish displaying signs of disease were markedly increased over-time in wild-type compared to heat-killed, fixed bacteria, and PBS controls (Figure 3B–D), suggesting that most of the pathogenic mechanisms require viability.

[¶] Carl Zeiss, Ostfildern, Germany

[#] GraphPad, San Diego, CA

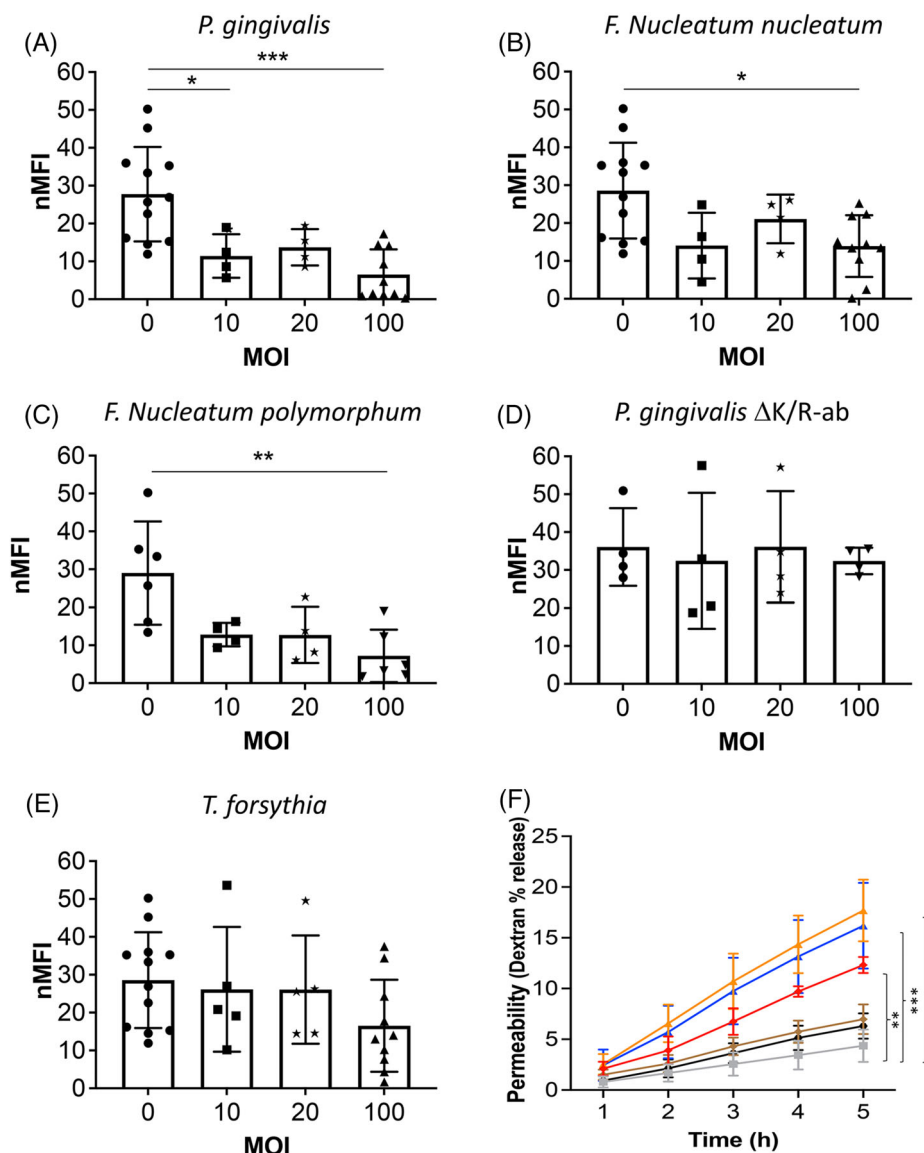


FIGURE 1 Reduction in PECAM-1 cell surface abundance and increase in endothelial monolayer permeability following *P. gingivalis* W83 and *F. nucleatum* infection. PECAM-1 cell surface abundance was measured by flow cytometric immunoassay after HMEC-1 were infected with (A) *P. gingivalis* strain W83, (B) *F. nucleatum* subspecies *nucleatum*, (C) *F. nucleatum* subspecies *polymorphum*, (D) *P. gingivalis* gingipain-null mutant Δ K/R-ab, or (E) *T. forsythia* at MOI 0, 10, 20, and 100. Data are presented as mean \pm SD of the normalized median fluorescence intensity (nMFI) of PECAM-1 following single species infection or uninfected control. Enclosed shapes represent data for each individual experiment ($n \geq 4$). (F) Permeability of HMEC-1 monolayers to fluorescently labeled 70 kDa dextran following treatment with different single species bacteria over 5 h. *F. nucleatum* subspecies *nucleatum* (orange), *F. nucleatum* subspecies *polymorphum* (blue), *P. gingivalis* strain W83 (red), *P. gingivalis* gingipain-null mutant Δ K/R-ab (brown), *T. forsythia* (black), Uninfected control (gray). Permeability data are presented as mean \pm SD dextran released into the lower transwell compartment of 3 independent experiments. Statistical differences in all experiments were analyzed by one-way ANOVA with Tukey's multiple comparison test. * $p < 0.05$ ** $p < 0.01$, *** $p < 0.001$

3.3 | *F. nucleatum* ssp *polymorphum* decreases PECAM-1 abundance and HMEC-1 viability more than ssp *nucleatum* in multispecies infection

For multispecies assessment, planktonic-grown *F. nucleatum* ssp *nucleatum* or ssp *polymorphum* were mixed with equal quantities with *P. gingivalis* W83 or *T. forsythia* (1:1,

MOI 100) or both (1:1:1, MOI 100) and their effects on HMEC-1 viability and PECAM-1 cell surface abundance measured (Figure 4). Multispecies infections containing *F. nucleatum* ssp *nucleatum* did not affect the viability of HMEC-1 cells when cultured in any combination of *P. gingivalis* W83 or *T. forsythia* (Figure 4A). In contrast, *F. nucleatum* ssp *polymorphum* induced significant ($p < 0.05$) HMEC-1 cell death when cultured with either

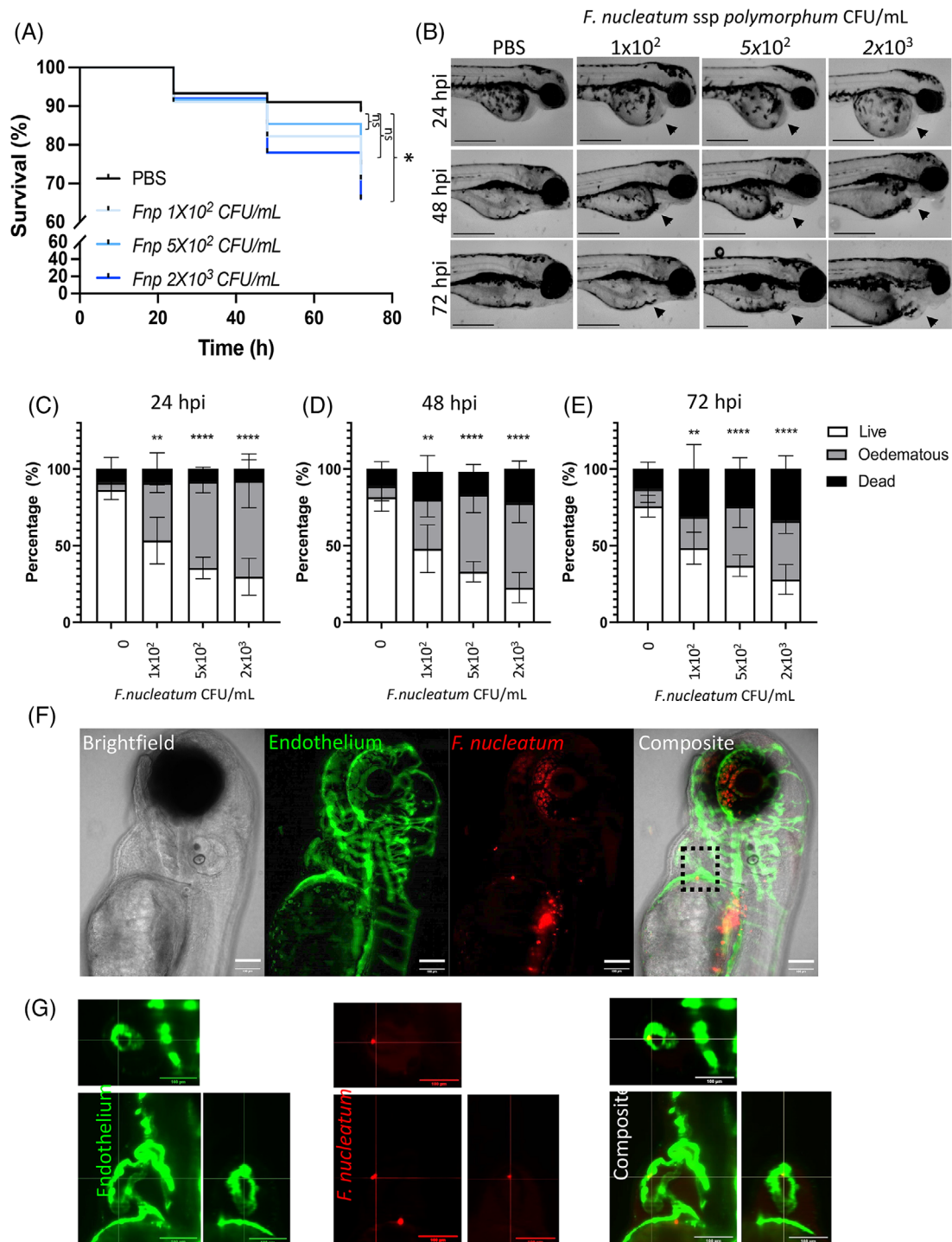


FIGURE 2 In vivo systemic infection of *F. nucleatum ssp polymorphum* results in increased zebrafish embryo mortality and morbidity. Zebrafish were injected with increasing amounts of *F. nucleatum ssp polymorphum* and mortality and morbidity measured. **(A)** Kaplan-Meier survival plot of zebrafish embryo infected at 30 hpf with PBS control or *F. nucleatum ssp polymorphum* (*Fnp*) at 1×10^2 , 5×10^2 , or 2×10^3 CFU/mL. Comparison of survival curves using the log-rank test shows significant differences between 2×10^3 CFU/mL *Fnp*-injected zebrafish and PBS controls at 72 hpi but no significant differences in survival at lower *Fnp* suspensions. **(B)** Representative micrographs showing the morphology of zebrafish larvae infected with PBS control, and increasing numbers of *Fnp* at 24, 48, and 72 hpi. *Fnp*-infected zebrafish showed marked edema around the yolk sac and heart (black arrows). Scale bars = 500 μ m. Percentage healthy, edematous, and dead zebrafish larvae at **(C)** 24, **(D)** 48, and **(E)** 72 hpi showing that the percentage of diseased (edematous + dead) zebrafish was significantly increased following systemic infection with *Fnp* at all time points. Data are presented as mean \pm SD of four independent experiments with a minimum of nine embryos per group. Statistical differences were analyzed by one-way ANOVA with Tukey's multiple comparison test. * $p < 0.05$, ** $p < 0.01$, **** $p < 0.0001$. **(F)** Lightsheet micrographs of *kdrl:mcherry* zebrafish embryo (green) from head to the yolk region following systemic injection

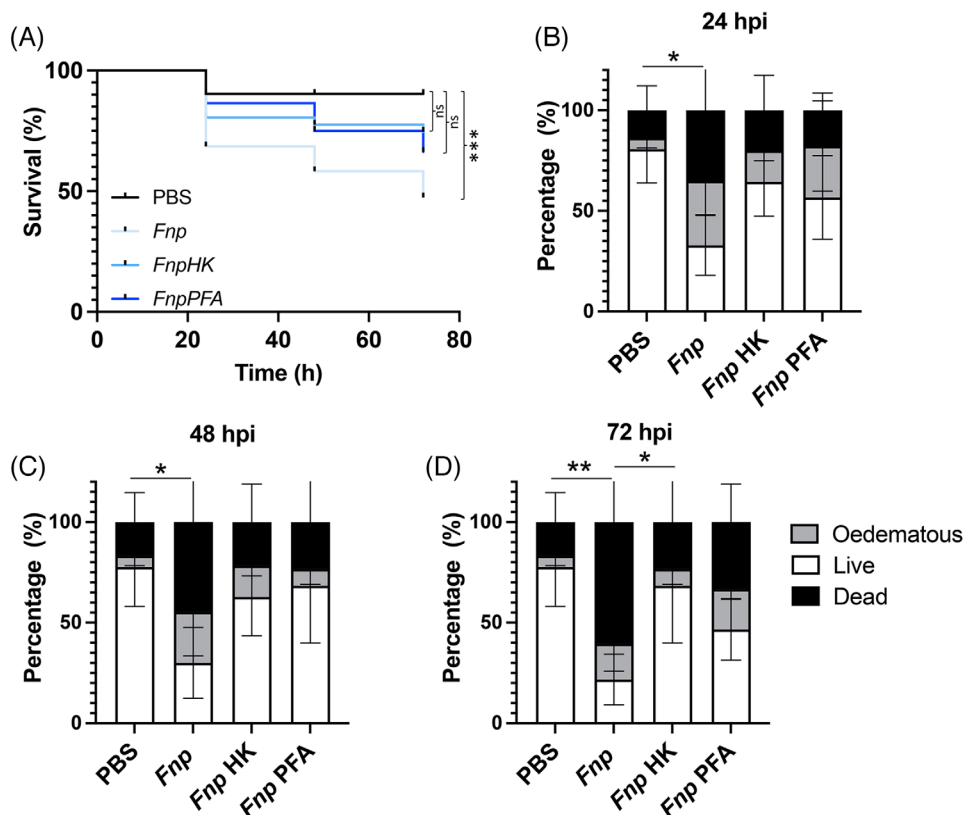


FIGURE 3 In vivo pathogenicity of *F. nucleatum* ssp *polymorphum* was significantly reduced after heat and paraformaldehyde fixative treatment. (A) Kaplan-Meier survival plots of zebrafish larvae infected 30 hpf with PBS control, *F. nucleatum* ssp *polymorphum* (*Fnp*), heat-killed *Fnp* (*FnpHK*), or paraformaldehyde-fixed (*FnpPFA*) bacteria, all at 2×10^3 CFU/ml. Comparison of survival curves using the log-rank test shows significant differences between *Fnp*-injected zebrafish compared to PBS controls at 72 hpi but no significant differences in survival in zebrafish injected with heat-killed or paraformaldehyde-fixed *F. nucleatum* *polymorphum*. Percentage healthy, edematous, and dead zebrafish larvae at (B) 24, (C) 48, and (D) 72 hpi zebrafish was significantly increased following systemic infection with *F. nucleatum* *polymorphum* at all time points. Data are presented as mean \pm SD of three independent experiments with a minimum of 10 embryos per group. Statistical differences were analyzed by one-way ANOVA with Tukey's multiple comparison test. * $p < 0.05$, ** $p < 0.01$, *** $p < 0.001$

P. gingivalis W83 or *T. forsythia* alone or as a mixture of all three bacteria compared to uninfected control (Figure 4B), suggesting that *F. nucleatum* ssp *polymorphum* is more virulent than ssp *nucleatum* when included in multispecies infection. Similarly, when included in multispecies infection, *F. nucleatum* ssp *nucleatum* did not significantly alter the cell surface abundance of PECAM-1 (Figure 4C), whereas multispecies cultures containing *F. nucleatum* ssp *polymorphum* were all able to cleave PECAM-1 causing its significant loss from HMEC-1 cells compared to uninfected controls (Figure 4D). Planktonic co-cultures of *P. gingivalis* W83 or *T. forsythia* significantly reduced PECAM-1 cell surface abundance on both occasions ($p < 0.05$, Figure 4C,D).

3.4 | PECAM-1 abundance and endothelium permeability changes are independent of gingipains when *F. nucleatum* ssp *polymorphum* is present in a mixed culture with *P. gingivalis*

Previous work has shown that *P. gingivalis* can cleave PECAM-1 in a gingipain-dependent manner.^{14,15} We, therefore, assessed the influence of gingipains on endothelial damage and permeability when wild-type *P. gingivalis* or its gingipain-null mutant Δ K/R-ab was combined with *F. nucleatum* ssp *polymorphum* and/or *T. forsythia*. Flow cytometric analysis showed a significant decrease

with 2 nl of 2×10^3 *Fnp* (red) and imaged at 2 hpi. Images were generated using SUM Z-projection function on FIJI® and show brightfield, vasculature, *Fnp* and composite images, respectively. (G) Orthogonal views of cardiac region (area indicated by the highlighted box in F). Right image, vasculature, center image *Fnp* and right composite image, further highlight the intravascular localization. Scale bars = 100 μ m

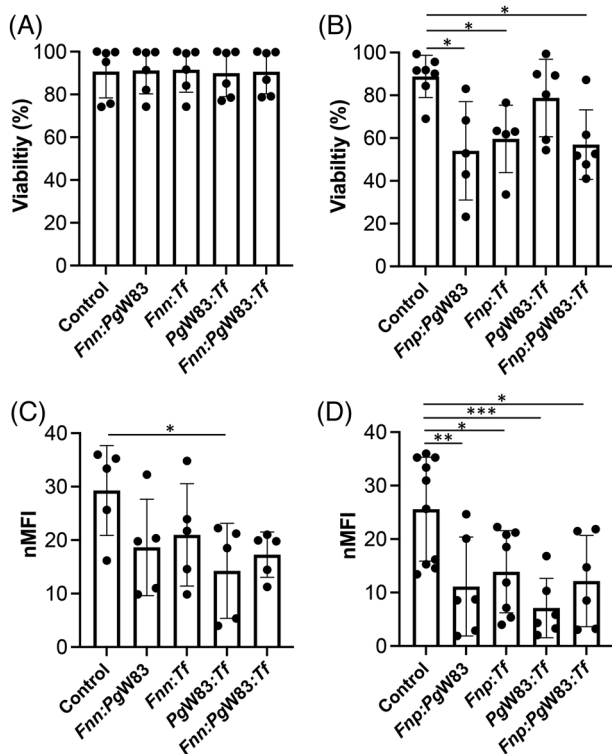


FIGURE 4 *F. nucleatum ssp polymorphum* decreases endothelial cell viability and PECAM-1 abundance in multispecies infections. HMEC-1 cells were infected for 1.5 h with multispecies bacterial co-cultures mixed in equal quantities of either *F. nucleatum ssp nucleatum* (*Fnn*) or *F. nucleatum ssp polymorphum* (*Fnp*) with either *P. gingivalis* W83 (*PgW83*) or *T. forsythia* (*Tf*) at 1:1 ratio or both at a 1:1:1 ratio. Total MOI was 100 in all treatments; controls received medium alone. HMEC-1 viability was determined by TO-PRO-3 staining for (A) *F. nucleatum ssp nucleatum* and (B) *F. nucleatum ssp polymorphum* and cell death calculated as a % of the total cell population. HMEC-1 cell surface abundance of PECAM-1 on live endothelial cells was determined by flow cytometry after multispecies infection containing (C) *F. nucleatum ssp nucleatum* and (D) *F. nucleatum ssp polymorphum*. Data are presented as normalized median fluorescence intensity (nMFI). In all graphs, enclosed circles represent data from each individual experiment and data are presented as mean \pm SD. Statistical differences were analyzed by one-way ANOVA with Dunnett's multiple comparison test. * $p < 0.05$, ** $p < 0.01$, *** $p < 0.001$

of PECAM-1 cell surface abundance ($p < 0.05$) when *F. nucleatum ssp polymorphum* was mixed with either wild-type *P. gingivalis* or the gingipain-deficient mutant (Figure 5A). Moreover, there was no significant difference when *F. nucleatum ssp polymorphum* was included in a co-culture with or without gingipains suggesting that there is no additive effect of PECAM-1 cleavage in the presence of gingipains (Figure 5A). Reduced PECAM-1 abundance was also observed when *F. nucleatum ssp polymorphum* or *P. gingivalis* was co-infected with *T. forsythia*, whereas the gingipain-null mutant, DK/R-ab, was not significantly

different when incubated with *T. forsythia*, suggesting that gingipains play a major role in PECAM-1 cleavage in *P. gingivalis* / *T. forsythia* mixed infections (Figure 5A). Similar findings were observed when HMEC-1 cells were infected with *F. nucleatum ssp polymorphum*, *P. gingivalis*, and *T. forsythia*, where PECAM-1 abundance was significantly decreased irrespective of the presence or absence of gingipains (Figure 5B). These results were once again mirrored when permeability was assessed using a dextran permeability assay (Figure 5C,D) were in both pairwise (Figure 5C) and triplicate mixed inoculates (Figure 5D) increased endothelial permeability in the presence of *F. nucleatum*. When inoculated systemically as a tri-mixture into zebrafish larvae, *F. nucleatum ssp polymorphum*, *P. gingivalis*, and *T. forsythia* were observed to be associated with the vasculature, particularly in the ocular and cardiac regions (Figure 6A–D) where fluorescence co-localization could be seen as the bacteria bind and aggregate with one another in vivo (Figure 6E–H). Hematoxylin and eosin-stained sagittal histological sections revealed advanced tissue damage in the cranial and gill filament regions along with yolk sac edemas compared to PBS-injected controls (Figure 6I,J).

4 | DISCUSSION

Although direct cause-effect evidence is to date still lacking⁵, the link between cardiovascular disease and periodontitis has been established by numerous studies.^{25,26} Chronic oral infection in periodontitis leads to entry of bacteria and/or their virulence factors into the bloodstream. This has been shown to cause vascular damage, partly through activation of the host inflammatory response through several mechanisms that potentiate atheromatous lesion formation, maturation, and exacerbation.^{11,27,28} Numerous oral microorganisms or their RNA/DNA have been identified in the vasculature including in atherosclerotic plaques²⁹ and periodontal pathogens identified vary depending on the bacterial identification method used.^{7,8}

P. gingivalis is as a keystone organism in periodontal disease.³⁰ This Gram-negative anaerobe has been recently described as the most abundant species in coronary and femoral arteries⁷ and can also dramatically increase morbidity and mortality of zebrafish in a gingipain-dependent manner after systemic injection.¹⁴ Among its many virulence factors attributed to causing vascular damage, gingipains appear to be the most important. Gingipains are lysine- and arginine-specific cysteine proteases that have the ability to cleave host proteins by mediating cell surface protein and extracellular matrix disruption.³¹ This in turn contributes to loss of cellular and tissue integrity.^{32–34} Even though *F. nucleatum* and *T. forsythia* are known

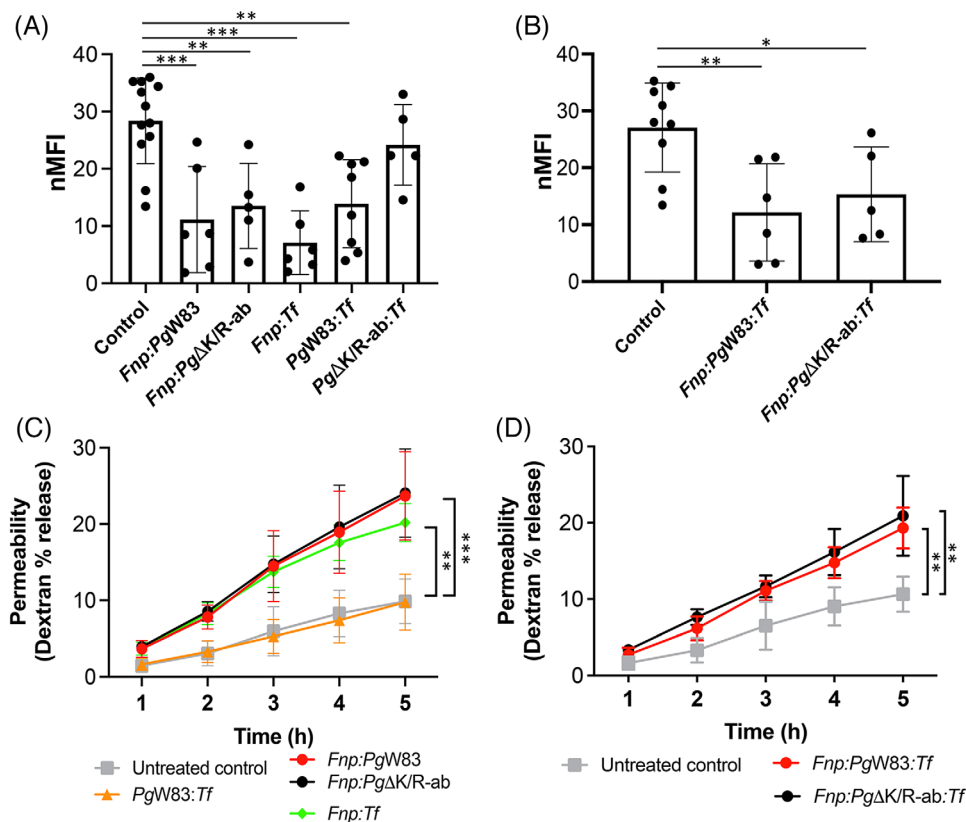


FIGURE 5 PECAM-1 abundance and permeability of HMEC-1 is independent of gingipain in multispecies infections. PECAM-1 cell surface abundance, as measured by flow cytometry, was decreased on viable HMEC-1 cells when treated with (A) pairwise combinations of *F. nucleatum* ssp *polymorphum* (*Fnp*), wild-type *P. gingivalis* W83 (PgW83), Gingipain-null *P. gingivalis* (Δ K/R-ab), or *T. forsythia* and (B) tri-mixtures of the same bacteria (Total MOI100). Data are presented as mean \pm SD normalized median fluorescence index (nMFI) with enclosed circles representing independent experiments. HMEC-1 monolayer permeability was measured using a dextran leakage assay. HMEC-1 permeability was measured after treatment with (C) pairwise combinations of *F. nucleatum* ssp *polymorphum* (*Fnp*), wild-type *P. gingivalis* W83 (PgW83), Gingipain-null *P. gingivalis* (Δ K/R-ab), or *T. forsythia* and (D) tri-mixtures of the same bacteria (Total MOI100). Permeability data are presented as mean \pm SD % dextran release of four independent experiments. In all experiments statistical significance was determined by a one-way analysis of variance with Tukey's post-hoc multiple comparisons test. * $p < 0.05$, ** $p < 0.01$, *** $p < 0.001$

periodontal pathobionts that have been identified in the vasculature and have also been shown to invade host cells,¹¹ their interaction with the endothelium is seldomly studied and even less their effects on endothelial adhesion molecule expression and permeability after polymicrobial infection.

Our data using single species infection mirror previously published data suggesting a gingipain-dependent reduction of PECAM-1, since no significant effects were noted in PECAM-1 levels and permeability after infection with the K/R-ab gingipain-null mutant.¹⁴ Single species infection with both *F. nucleatum* ssp *polymorphum* or *F. nucleatum* ssp *nucleatum* resulted in similar endothelial damage to that observed following wild-type *P. gingivalis* (strain W83) infection. Like *P. gingivalis*, *F. nucleatum* is known for its capability of living in hostile environments,³⁵ and although *F. nucleatum* does not produce gingipains, it produces several virulence factors including serine

proteases.³⁶ PECAM-1 reduction following infection with *F. nucleatum* ssp *nucleatum* (ATCC 25586) has been previously reported on human umbilical vein endothelial cells (HUVEC) using the same MOI as reported in this study but at longer infection times of 4–24 h.¹⁶ *F. nucleatum* ssp *nucleatum* was also found to induce proinflammatory changes, increase vascular endothelial growth factor (VEGF) release and suppression of endothelial cell proliferation, indicating that *F. nucleatum* ssp *nucleatum* may also have a pivotal role in mediating vascular damage.¹⁶

Experiments using monolayer cultures of endothelial cells provide informative data, but these experiments lack conditions such as flow and shear stress that are important features in systemic infection. Zebrafish have been extensively used for host-pathogen interactions and have several advantages such as transparency and availability of fluorescently tagged proteins that allow for real-time analysis of cell–cell interactions. Moreover, the close genomic

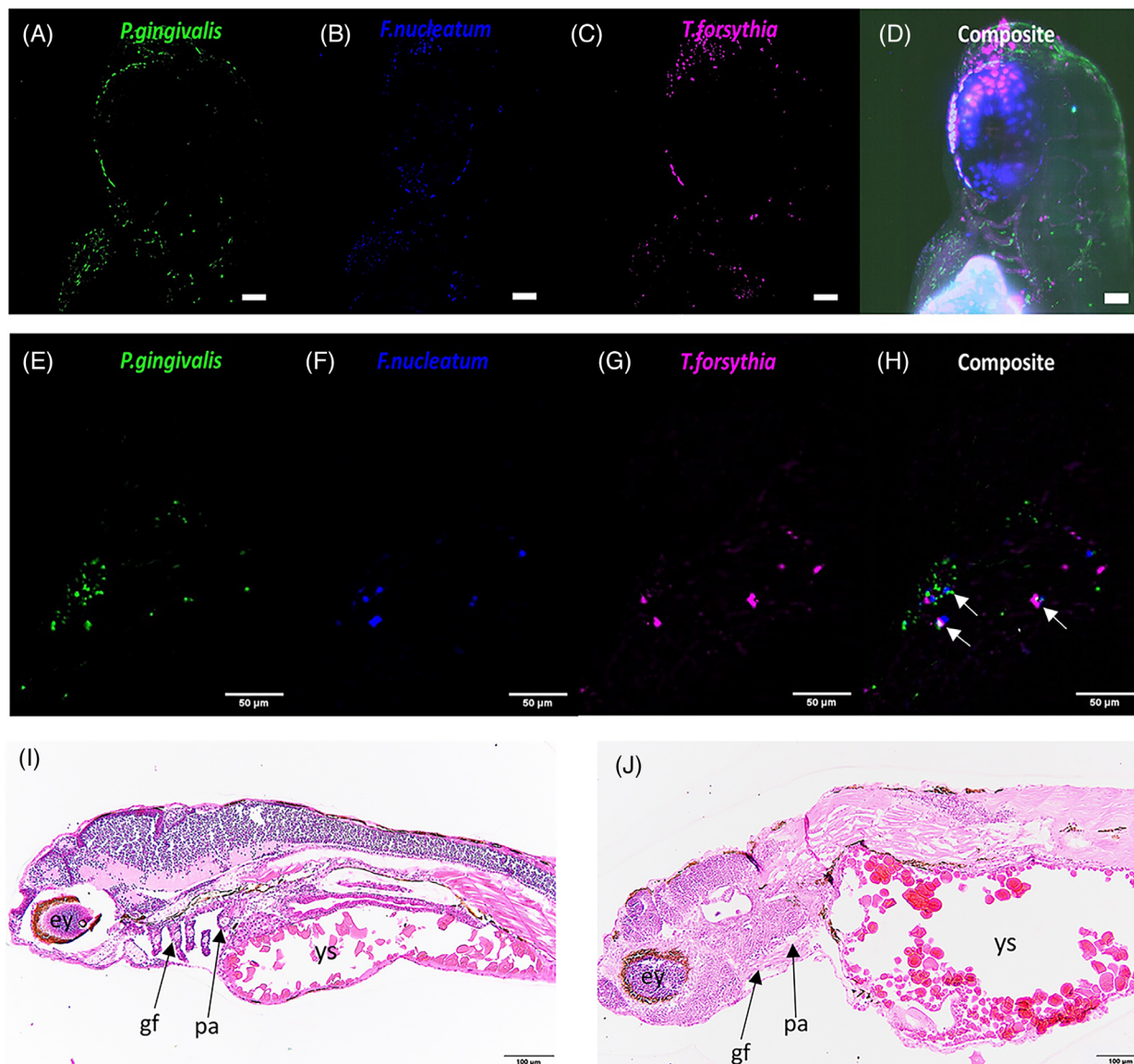


FIGURE 6 Multispecies dissemination of periodontal pathogens in vivo. Maximum intensity projections generated 2 hpi of Nacre zebrafish embryo. 48 hpf zebrafish embryos were injected with 2 nl of a multispecies inoculum containing 5(6)-FAM, SE-labeled *P. gingivalis* W83 (green), Cell Tracker® CMPTX-labeled *F. nucleatum* ssp *polymorphum* (false-colored blue) and Cell Tracker® Deep Red-labeled *T. forsythia* (false-colored magenta) in the common cardinal vein at 2×10^3 total CFU/ml. (A–D) Fluorescence micrographs of the head and cardiac region showing systemic dissemination of all three species in separate fluorescence channels (A–C) followed by a composite image (D). (E–H) Maximum intensity projection micrographs at higher magnification in cardiac region of zebrafish embryo. (E–G) Separate channel micrographs showing the vascular distribution of (E) *P. gingivalis*, (F) *F. nucleatum* ssp *polymorphum*, and (G) *T. forsythia*. (H) Depicts a composite image where the white arrows highlight colocalization of different bacterial species. Scale bar = 50 μ m. Hematoxylin and eosin-stained sagittal histological sections of (I) PBS-injected and (J) multispecies (*P. gingivalis*, *F. nucleatum* ssp *polymorphum*, *T. forsythia*)-injected zebrafish embryo. Tissue damage and cellular necrosis can be observed in the multi-species-injected zebrafish embryo within the cranial and ocular region (ey), gill filaments (gf), and pharyngeal arch (pa), along with an enlarged yolk sac (ys) due to excessive edema

homology to humans and use of similar host defense pathways means that this in vivo model system is ideally placed to examine systemic bacterial infection.³⁷ Indeed, we have used this model to identify the molecular mechanisms at play during systemic *P. gingivalis* infection.^{34,38} This study is the first to show *F. nucleatum* ssp *polymorphum* is able

to cause significant in vivo mortality when injected systemically in a zebrafish model, with virulence similar to that observed for *P. gingivalis* in terms of overall disease morbidity.³⁴

T. forsythia infection did not result in significant changes in PECAM-1 abundance or endothelial permeability at



the time frames used in our experiments. These data align with previous animal studies where infection with *T. forsythia* did not affect atherosclerotic lesion size, although an increase in inflammatory modulators was observed.³⁹ The authors concluded that different organisms may contribute to vascular damage at different stages or that organisms exhibit different virulence potential when present as a single species.³⁹ Lack of polymicrobial research in this area along with animal studies that have highlighted that the pathogenic effects on the vasculature might differ in single versus multi species infection led us to further investigate the effects of polymicrobial infections on endothelial cells.

P. gingivalis is generally found associated with other pathogens and not as a solitary organism,¹⁸ while *F. nucleatum* infections also often involve multiple species.⁴⁰ Therefore investigation of their pathogenic effects when interacting with other species is important. Previous research has shown that *P. gingivalis* enhances the attachment of *T. forsythia* to epithelial cells, enhancing its invasion.⁴¹ Our data showed that pairing *P. gingivalis* with *T. forsythia* increased the virulence of *T. forsythia*. Although decrease in PECAM-1 abundance was not uniformly statistically significant in all experiments performed, indicating that higher MOI or longer infection times might be required for effects to be more uniform. *F. nucleatum* ssp *nucleatum* enhanced the invasion of *P. gingivalis* into both gingival epithelial and aortic endothelial cells,¹⁹ while contrastingly, another study showed that *P. gingivalis* suppressed invasion of coinfecting *F. nucleatum* ssp *nucleatum* in gingival epithelial cells with gingipain-mediated inactivation of the PI3K/AKT pathway suggested as a possible reason.⁴⁰ This particular microbial interaction may be a reason why reduction in PECAM-1 abundance was only observed with polymicrobial infections containing *P. gingivalis* and *F. nucleatum* ssp *polymorphum* and not *F. nucleatum* ssp *nucleatum*.

These data highlight differences in virulence between *F. nucleatum* ssp *nucleatum* and ssp *polymorphum*. In single species infection, *F. nucleatum* ssp *nucleatum* and ssp *polymorphum* both caused a significant decrease in PECAM-1 abundance. When mixed pairwise with other bacteria, *F. nucleatum* ssp *nucleatum* was less virulent than ssp *polymorphum* in terms of HMEC-1 viability and PECAM-1 loss, suggesting that different *F. nucleatum* subspecies might display varying amounts of virulence factors. Although *F. nucleatum* ssp *nucleatum* and ssp *polymorphum* share many highly conserved genes whose products are associated with bacteria-to-bacteria and bacteria-to-host cell adhesion and virulence (such as FadA,⁴² RadD,⁴³ Fap2,⁴⁴ and FomA⁴⁵), 25% of the open-reading frames in ssp *polymorphum* (ATCC10953) are not represented in other *Fusobacterium* and several of these unique genes

code for virulence factors.⁴⁶ There are also differences in the carbohydrate moieties on the lipopolysaccharide (LPS) O-antigen between *F. nucleatum* ssp, with ssp *polymorphum* (ATCC 10953) containing sialic acid as a constituent of its O-antigen, whereas this is lacking in ssp *nucleatum* (ATCC 25586).^{47,48} Moreover, the protease fusolisins has been identified in both *F. nucleatum* subspecies, however its expression and secretion markedly varies between strains.⁴⁹ These subtle inter-strain variances may explain the differences between the two strains in terms of virulence toward endothelial cells, in both single species as well as multi-species infection.

The reduction of PECAM-1 abundance following co-infection of *F. nucleatum* ssp *polymorphum* with *P. gingivalis* in the presence (wild-type) or absence (K/R-ab) of gingipain was similar. This is interesting because it might be expected that *F. nucleatum* proteases and gingipains would act in concert to produce enhanced PECAM-1 degradation. It could be that the *F. nucleatum* proteases have higher affinity or are more active meaning that their degradative effects override that of gingipains or that these enzymes are in competition during co-infection, limiting their individual effects. The addition of *T. forsythia* appears to have no additional effect in polymicrobial infection. Similar observations were shown in polymicrobial biofilm formation by other authors,⁵⁰ but, to date, there are no studies showing protease effects on the vasculature in polymicrobial infections.

It is unclear whether *F. Nucleatum* ssp *polymorphum* might play a greater role than *P. gingivalis* in vascular damage. *P. gingivalis* has been claimed to guide *F. nucleatum* to a paracellular pathway,⁴⁰ potentially increasing its virulence. Another hypothesis is that arginine-inhibitable adhesins produced by *F. nucleatum*⁴³ alter gingipain activity, thereby reducing *P. gingivalis* virulence. These findings highlight the potential role of *F. nucleatum* in both single species and polymicrobial interactions on vascular damage. This research also further asserts the need for a broader approach in the investigation of periodontal pathogen interactions with the vasculature since these organisms might behave or respond to treatment differently if in close proximity or attached to one another.

5 | CONCLUSIONS

Here, we show that *F. nucleatum*, in particular ssp *polymorphum*, affects endothelial adhesion molecule abundance, cell viability, and vascular permeability, even when part of polymicrobial infection. The results highlight the need for further research on potential mechanisms of cardiovascular damage following polymicrobial infections involving *F. nucleatum* strains and the role these



interspecies interactions play in their potential pathogenic effects on the endothelium.

ACKNOWLEDGMENTS

The authors acknowledge Darren Robinson and Nick van Hateren (Wolfson Light Microscopy Facility, University of Sheffield) for help with in vivo imaging. The Wolfson Light Microscopy Facility is supported by a Biotechnology and Biological Sciences Research Council, UK (BBSRC) ALERT14 award (BB/M012522/1). This work was supported by the Oral and Dental Research Trust, UK (CM, CF) and British Society of Periodontology Research Award, UK (CF). CF is the recipient of a University of Sheffield Faculty Studentship.

CONFLICTS OF INTEREST

The authors declare no conflict of interest.

AUTHOR CONTRIBUTIONS

Cher Farrugia, Graham P. Stafford, and Craig Murdoch conceived, designed the research and planned experiments. Cher Farrugia, Ashley F. Gains, and Antonia R. Cutts performed the experiments, while Cher Farrugia and Craig Murdoch analyzed the data, conducted statistical analysis, and interpreted the results. Cher Farrugia wrote the manuscript draft, and further editing was performed by Graham P. Stafford and Craig Murdoch.

ORCID

Craig Murdoch  <https://orcid.org/0000-0001-9724-122X>

REFERENCES

- Gustafsson N, Ahlqvist J, Naslund U, et al. Associations among periodontitis, calcified carotid artery atheromas, and risk of myocardial infarction. *J Dent Res* 2020;99:60-68.
- Kebschull M, Demmer RT, Papapanou PN. "Gum bug, leave my heart alone!"-epidemiologic and mechanistic evidence linking periodontal infections and atherosclerosis. *J Dent Res* 2010;89:879-902.
- Castillo DM, Sanchez-Beltran MC, Castellanos JE, et al. Detection of specific periodontal microorganisms from bacteraemia samples after periodontal therapy using molecular-based diagnostics. *J Clin Periodontol* 2011;38:418-427.
- Loos BG. Systemic markers of inflammation in periodontitis. *J Periodontol* 2005;76(11S):2106-2115.
- Herrera D, Molina A, Buhlin K, Klinge B. Periodontal diseases and association with atherosclerotic disease. *Periodontol* 2000;2000;83:66-89.
- Gaetti-Jardim E, Marcelino SL, Feitosa ACR, Romito GA, Avila-Campos MJ. Quantitative detection of periodontopathic bacteria in atherosclerotic plaques from coronary arteries. *J Med Microbiol* 2009;58:1568-1575.
- Mougeot JC, Stevens CB, Paster BJ, Brennan MT, Lockhart PB, Mougeot FK. *Porphyromonas gingivalis* is the most abundant species detected in coronary and femoral arteries. *J Oral Microbiol* 2017;9:1281562.
- Marin MJ, Figuero E, Gonzalez I, et al. Comparison of the detection of periodontal pathogens in bacteraemia after tooth brushing by culture and molecular techniques. *Med Oral Patol Oral Cir Bucal* 2016;21:e276-e284.
- Marcelino SL, Gaetti-Jardim E, Jr., Nakano V, et al. Presence of periodontopathic bacteria in coronary arteries from patients with chronic periodontitis. *Anaerobe* 2010;16:629-632.
- Lockhart PB, Brennan MT, Sasser HC, Fox PC, Paster BJ, Bahrani-Mougeot FK. Bacteremia associated with toothbrushing and dental extraction. *Circulation* 2008;117:3118-3125.
- Reyes L, Herrera D, Kozarov E, Roldan S, Progulske-Fox A. Periodontal bacterial invasion and infection: contribution to atherosclerotic pathology. *J Clin Periodontol* 2013;40(14):S30-S50.
- Zhang J, Xie M, Huang X, et al. The effects of *Porphyromonas gingivalis* on atherosclerosis-related cells. *Front Immunol* 2021;12:766560.
- Privratsky JR, Newman PJ. PECAM-1: regulator of endothelial junctional integrity. *Cell Tissue Res* 2014;355:607-619.
- Widziolek M, Prajsnar TK, Tazyman S, Stafford GP, Potempa J, Murdoch C. Zebrafish as a new model to study effects of periodontal pathogens on cardiovascular diseases. *Sci Rep* 2016;6:36023.
- Yun PL, Decarlo AA, Chapple CC, Hunter N. Functional implication of the hydrolysis of platelet endothelial cell adhesion molecule 1 (CD31) by gingipains of *Porphyromonas gingivalis* for the pathology of periodontal disease. *Infect Immun* 2005;73:1386-1398.
- Mendes RT, Nguyen D, Stephens D, et al. Endothelial cell response to *Fusobacterium nucleatum*. *Infect Immun* 2016;84:2141-2148.
- Fardini Y, Wang X, Temoin S, et al. *Fusobacterium nucleatum* adhesin FadA binds vascular endothelial cadherin and alters endothelial integrity. *Mol Microbiol* 2011;82:1468-1480.
- Yao ES, Lamont RJ, Leu SP, Weinberg A. Interbacterial binding among strains of pathogenic and commensal oral bacterial species. *Oral Microbiol Immunol* 1996;11:35-41.
- Saito A, Inagaki S, Kimizuka R, et al. *Fusobacterium nucleatum* enhances invasion of human gingival epithelial and aortic endothelial cells by *Porphyromonas gingivalis*. *FEMS Immunol Med Microbiol* 2008;54:349-355.
- Chukkapalli SS, Velsko IM, Rivera-Kweh MF, Zheng D, Lucas AR, Kesavalu L. Polymicrobial oral infection with four periodontal bacteria orchestrates a distinct inflammatory response and atherosclerosis in ApoE null mice. *PLoS One* 2015;10:e0143291.
- Nahid MA, Rivera M, Lucas A, Chan EK, Kesavalu L. Polymicrobial infection with periodontal pathogens specifically enhances microRNA miR-146a in ApoE^{-/-} mice during experimental periodontal disease. *Infect Immun* 2011;79:1597-1605.
- Velsko IM, Chukkapalli SS, Rivera-Kweh MF, et al. Periodontal pathogens invade gingiva and aortic adventitia and elicit inflammasome activation in $\alpha\beta6$ integrin-deficient mice. *Infect Immun* 2015;83:4582-4593.
- Ades EW, Candal FJ, Swerlick RA, et al. HMEC-1: establishment of an immortalized human microvascular endothelial cell line. *J Invest Dermatol* 1992;99:683-690.



24. Wang Y, Alexander JS. Analysis of endothelial barrier function in vitro. *Methods Mol Biol* 2011;763:253-264.
25. Friedewald VE, Kornman KS, Beck JD, et al. The American Journal of Cardiology and Journal of Periodontology: periodontitis and atherosclerotic cardiovascular disease. *Am J Cardiol* 2009;104:59-68.
26. Sanz M, Marco Del Castillo A, Jepsen S, et al. Periodontitis and cardiovascular diseases: consensus report. *J Clin Periodontol* 2020;47:268-288.
27. Tonetti MS, Van Dyke TE. working group 1 of the joint EFPAAAPw. Periodontitis and atherosclerotic cardiovascular disease: consensus report of the Joint EFP/AAPWorkshop on Periodontitis and Systemic Diseases. *J Periodontol* 2013;84(4S):S24-S29.
28. Schenkein HA, Papapanou PN, Genco R, Sanz M. Mechanisms underlying the association between periodontitis and atherosclerotic disease. *Periodontol 2000* 2020;83:90-106.
29. Chiu B. Multiple infections in carotid atherosclerotic plaques. *Am Heart J* 1999;138:S534-536.
30. Hajishengallis G, Darveau RP, Curtis MA. The keystone-pathogen hypothesis. *Nat Rev Microbiol* 2012;10:717-725.
31. Hocevar K, Potempa J, Turk B. Host cell-surface proteins as substrates of gingipains, the main proteases of *Porphyromonas gingivalis*. *Biol Chem* 2018;399:1353-1361.
32. Tada H, Sugawara S, Nemoto E, et al. Proteolysis of ICAM-1 on human oral epithelial cells by gingipains. *J Dent Res* 2003;82:796-801.
33. Ruggiero S, Cosgarea R, Potempa J, Potempa B, Eick S, Chiquet M. Cleavage of extracellular matrix in periodontitis: gingipains differentially affect cell adhesion activities of fibronectin and tenascin-C. *Biochim Biophys Acta* 2013;1832:517-526.
34. Farrugia C, Stafford GP, Potempa J, et al. Mechanisms of vascular damage by systemic dissemination of the oral pathogen *Porphyromonas gingivalis*. *FEBS J* 2021;288:1479-1495.
35. de Andrade KQ, Almeida-da-Silva CLC, Coutinho-Silva R. Immunological pathways triggered by *Porphyromonas gingivalis* and *Fusobacterium nucleatum*: therapeutic possibilities? *Mediators Inflamm* 2019;2019:7241312.
36. Bachrach G, Rosen G, Bellalou M, Naor R, Sela MN. Identification of a *Fusobacterium nucleatum* 65 kDa serine protease. *Oral Microbiol Immunol* 2004;19:155-159.
37. Gomes MC, Mostowy S. The case for modeling human infection in zebrafish. *Trends Microbiol* 2020;28:10-18.
38. Farrugia C, Stafford GP, Murdoch C. *Porphyromonas gingivalis* outer membrane vesicles increase vascular permeability. *J Dent Res* 2020;99:1494-1501.
39. Chukkapalli SS, Rivera-Kweh MF, Velsko IM, et al. Chronic oral infection with major periodontal bacteria *Tannerella forsythia* modulates systemic atherosclerosis risk factors and inflammatory markers. *Pathog Dis* 2015;73.
40. Jung YJ, Jun HK, Choi BK. *Porphyromonas gingivalis* suppresses invasion of *Fusobacterium nucleatum* into gingival epithelial cells. *J Oral Microbiol* 2017;9:1320193.
41. Inagaki S, Onishi S, Kuramitsu HK, Sharma A. *Porphyromonas gingivalis* vesicles enhance attachment, and the leucine-rich repeat BspA protein is required for invasion of epithelial cells by *Tannerella forsythia*. *Infect Immun* 2006;74:5023-5028.
42. Han YW, Ikegami A, Rajanna C, et al. Identification and characterization of a novel adhesin unique to oral fusobacteria. *J Bacteriol* 2005;187:5330-5340.
43. Kaplan CW, Lux R, Haake SK, Shi W. The *Fusobacterium nucleatum* outer membrane protein RadD is an arginine-inhibitable adhesin required for inter-species adherence and the structured architecture of multispecies biofilm. *Mol Microbiol* 2009;71:35-47.
44. Kaplan CW, Ma X, Paranjpe A, et al. *Fusobacterium nucleatum* outer membrane proteins Fap2 and RadD induce cell death in human lymphocytes. *Infect Immun* 2010;78:4773-4778.
45. Jensen HB, Skeidsvoll J, Fjellbirkeland A, et al. Cloning of the fomA gene, encoding the major outer membrane porin of *Fusobacterium nucleatum* ATCC10953. *Microb Pathog* 1996;21:331-342.
46. Karpathy SE, Qin X, Gioia J, et al. Genome sequence of *Fusobacterium nucleatum* subspecies *polymorphum* – a genetically tractable fusobacterium. *PLoS One* 2007;2:e659.
47. Vinogradov E, St Michael F, Cox AD. The structure of the LPS O-chain of *Fusobacterium nucleatum* strain 25586 containing two novel monosaccharides, 2-acetamido-2,6-dideoxy-l-altrose and a 5-acetimidoamino-3,5,9-trideoxy-gluco-non-2-ulosonic acid. *Carbohydr Res* 2017;440-441:10-15.
48. Vinogradov E, St Michael F, Homma K, Sharma A, Cox AD. Structure of the LPS O-chain from *Fusobacterium nucleatum* strain 10953, containing sialic acid. *Carbohydr Res* 2017;440-441:38-42.
49. Doron L, Copenhagen-Glazer S, Ibrahim Y, et al. Identification and characterization of fusolisins, the *Fusobacterium nucleatum* autotransporter serine protease. *PLoS One* 2014;9:e111329.
50. Bao K, Belibasakis GN, Thurnheer T, Aduse-Opoku J, Curtis MA, Bostanci N. Role of *Porphyromonas gingivalis* gingipains in multi-species biofilm formation. *BMC Microbiol* 2014;14:258.

How to cite this article: Farrugia C, Stafford GP, Gains AF, Cutts AR, Murdoch C. *Fusobacterium nucleatum* mediates endothelial damage and increased permeability following single species and polymicrobial infection. *J Periodontol*. 2022;93:1421-1433.

<https://doi.org/10.1002/JPER.21-0671>